Analysis of a Novel Switched-Flux Memory Motor Employing Time-Divisional Magnetization Strategy

Hui Yang, Heyun Lin*, *Member*, *IEEE*, Jianning Dong, Jianhu Yan, Yunkai Huang and Shuhua Fang
Engineering Research Center for Motion Control of Ministry of Education, Southeast University, Nanjing 210096, China
* hyling@seu.edu.cn

***Abstract*—This paper presents a novel switched-flux memory motor (SFMM) by incorporating the flux-mnemonic concept into the conventional switched-flux permanent magnet machine (SFPMM). The magnetic susceptibility of AlNiCo PM provides the flexible online controllability of air-gap flux by imposing a transient current pulse, which is extremely applicable for electric vehicle (EV) drives. To uniformize magnetization levels of PMs, a time-divisional magnetization strategy (TDMS) is proposed. Due to the uniqueness of hysteresis nonlinearity and instability regarding AlNiCo PM operating point, the time-stepping finite element method (TSFEM) dynamically coupled with a nonlinearity-involved parallelogram hysteresis model (NIPHM) of AlNiCo PM is performed to investigate the electromagnetic performance of the proposed SFMM, where the prediction is quantitatively compared with the counterpart integrated with the PHM and verifies the flux-adjustable capability of the proposed machine equipped with TDMS and the validity of the developed NIPHM.**

***Index Terms*—Magnetization, memory motor, permanent magnet, switched-flux**

I. Introduction

Memory motor, a new embranchment of genuinely variable flux permanent magnet machine (VFPMM) adopting AlNiCo PMs with intrinsical low coercivity and high remanence, is predominantly desirable for modern EV drives since it achieves prominent flux-adjusting capability at the cost of negligible excitation loss [1].

This paper proposes a novel switched-flux memory motor (SFMM) by incorporating the flux-mnemonic concept into the switched-flux PM motor (SFPMM) [2], which artfully combines noticeable electromagnetic performance exhibited in SFPMM and remarkable flux controllability of memory machine [3-5]. Besides, a time-divisional magnetization strategy is presented to avoid the unequal magnetization levels of PMs caused by the rotation of rotor. A nonlinearity-involved parallelogram hysteresis model (NIPHM) accounting for the saturated magnetization of AlNiCo PM is developed to simplify the repetitive PM magnetization/demagnetization process for numerical analysis. The numerical analysis using the time-stepping finite element method (TSFEM) coupled with the NIPHM is accomplished to predict the electromagnetic performance of the SFMM. The analysis results verify the flux-adjustable capability of the proposed SFMM and the effectiveness of the NIPHM. Fig. 1 depicts the cross-sectional view of a three-phase 12/10-pole SFMM configuration. In the stator, the circumferentially magnetized AlNiCo PMs with alternative-polarity are embedded in the "U"-shape laminated stator segments, while the magnetizing coils are accommodated in the outer slots adjacent to the PMs and the air-gap bridges are built in the external layer of the stator yoke to reduce the PM flux leakage. The salient-pole rotor is simply manufactured by the laminated silicon steel sheets. The proposed SFMM not only inherits high torque capability, structural robustness, flux-concentrating features and sinusoidal back-EMF waveform desirable for brushless AC operation.

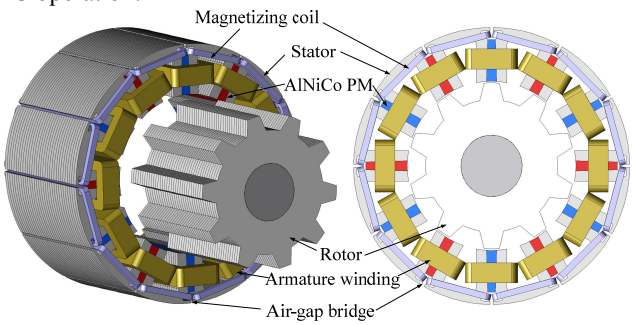

Fig. 1. Proposed 12/10-pole SFMM. (a) Cutaway view. (b) Cross-sectional view.

II. Time-Divisional Magnetization Strategy

To uniformize the magnetization levels of PMs, which are affected by rotor position, a time-divisional magnetization strategy is presented, in which the current pulses are in turn imposed in the magnetizing coils. The magnetization control scheme and the idealized magnetized or demagnetized locality, which is confirmed to tune the magnetization levels of the AlNiCo PMs properly over an electrical period, are respectively addressed in Fig. 2. The flux control circuit consists of a controllable voltage source with *H*-bridge converter and a Buck converter. The former determines the directions of pulse currents and the energizing sequence of magnetizing coils; while the latter governs the magnitudes of temporary current pulses.

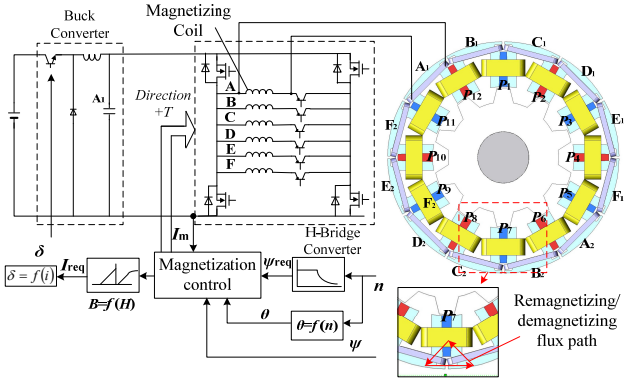

Fig. 2. The Block diagram of time-divisional magnetization control and optimal PM magnetization locality.

III. Implementation of TSFEM Coupled with NIPHM

The NIPHM of AlNiCo PM is illustrated in Fig. 3, where the major hysteresis loops and all the minor loops are hypothetically blessed with identical value of coercivity H_c, but different values of remanence B_{rk}. The set of parallel minor loop lines labeled with l_1 can be expressed as:

$$B = \mu_0 \mu_r H_m + B_{rk}, \quad n = 1, 2, 3\ldots . \tag{1}$$

where μ_0 and μ_r are the vacuum permeability and the relative permeability of AlNiCo PM, respectively; H_m is the positive magnetic field intensity, and B_{rk} represents the corresponding k^{th} remanence of the sets of hysteresis loops.

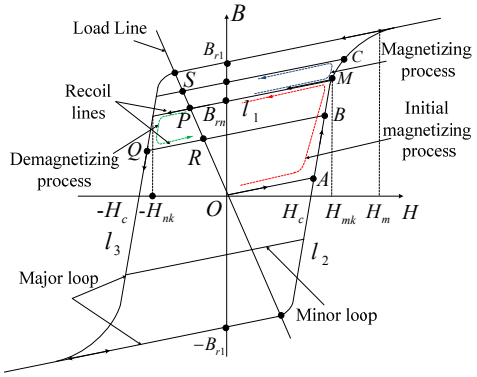

Fig. 3. NIPHM of AlNiCo PM.

The common two profiles of the major loop and the minor loop can be fitted into 3-order nonlinear functions, where l_2 and l_3 can be respectively expressed as:

$$H = f(B) = A_0 + A_1 B + A_2 B^2 + A_3 B^3 . \tag{2}$$

$$H = -f(-B) = -A_0 + A_1 B - A_2 B^2 + A_3 B^3 . \tag{3}$$

where the coefficients can be determined by experimentally statistical fitting.

During the magnetizing initialization, when applying a temporary flux intensity H_0, the operating point will move along *OAMP* and stabilizes at point *P*, where the corresponding remanence B_{rP} can be derived as:

$$B_{rP} = \begin{cases} 0, & 0 \le H_0 \le H_c \\ f^{-1}(H_0) - \mu_r \mu_0 H_0 , & H_c \le H_0 \le H_m \\ B_{r1}, & H_m \le H_0 \end{cases} \tag{4}$$

During the flux-adjustment stage, if a remagnetizing pulsating flux intensity H is applied, the operating point will shift along *PMCS* and settle at *S* with the relevant remanence B_{rS} deduced as:

$$B_{rS} = \begin{cases} 0, & 0 \le H \le H_c \\ f^{-1}(H) - \mu_r \mu_0 H , & H_{mk} \le H \le H_m \\ B_{r1}, & H_m \le H \end{cases} . \tag{5}$$

During the demagnetizing status, the operating point will track along *PQR* and finally arrive at point *R* with the corresponding remanence B_{rR} deduced as:

$$B_{rR} = \begin{cases} B_{rk} & H_{nk} \le H \le 0 \\ -f^{-1}(-H) - \mu_r \mu_0 H , & -H_m \le H \le -H_{nk} \\ -B_{r1} & H \le -H_m \end{cases} \tag{6}$$

IV. Performance Prediction

By adopting the TSFEM coupled with the NIPHM, the magnetic field distributions under the different magnetization pulse currents are calculated and shown in Fig. 4. It can be observed that the no-load magnetization of PMs can be tuned flexibly by temporarily applying the various pulse currents with the peak values of +10A, +4A, -3A, -5A, respectively.

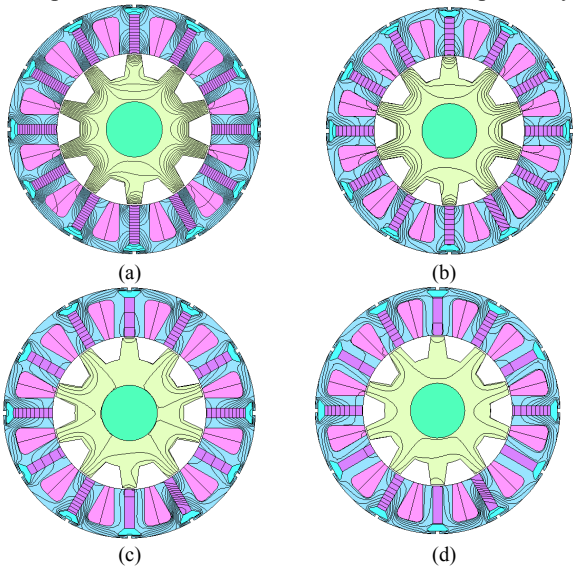

Fig. 4. Open-circuit magnetic field distributions under different current pulses. (a) +10A. (b) +4A. (c) -3A. (d) -5A.

V. Conclusion

This paper proposes a novel three-phase 12/10-pole SFMM equipped with a time-divisional online magnetization strategy, which not only retains remarkable online flux controllability, but also inherits the applicability for brushless AC operation in conventional SFPMM. The electromagnetic performance of the proposed motor is successfully predicted by the TSFEM coupled with the NIPHM, which involves the saturated magnetization of PM elements. The analysis results verify the flux-adjusting ability of the proposed motor and the effectiveness of the proposed computational method.

In the full-paper, a detailed description regarding the combinative algorithm and performance evaluation of the motor will be presented to verify the analysis.

References

[1] V. Ostovic, "Memory motors: A new class of controllable-flux permanent magnet machines for true wide-speed operation," *IEEE Ind. Appl. Mag.*, vol. 9, no. 1, pp. 52–61, Jan./Feb. 2003.

[2] Z. Q. Zhu and J. T. Chen, "Advanced flux-switching permanent magnet brushless machines," *IEEE Trans. on Magn.*, vol. 46, no.6, pp. 1447-1453, 2010.

[3] Liu Hengchuan, Lin Heyun, Fang Shuhua, and Z. Q. Zhu, "Permanent magnet demagnetization physics of a variable flux memory motor," *IEEE Trans. on Magn.*, vol. 45, no.10, pp. 4736-4739, 2009.

[4] Liu Hengchuan, Lin Heyun, Z. Q. Zhu, Huang Mingming, and Jin Ping, "Permanent magnet remagnetizing physics of a variable flux memory motor," *IEEE Trans. on Magn.*, vol. 46, no.6, pp. 1679-1682, 2010.

[5] Y. G. Chen, W. Pan, Y. H. Shen, and R. Y. Tang, "Interior composite-rotor controllable-flux PMSM-memory motor," in *Proc. Conf. Rec. ICEMS'05*, 2005, pp. 446–449.